Kinetic Model for Positive Tone Resist Dissolution and Roughening

F. A. Houle,* W. D. Hinsberg,* and M. I. Sanchez

IBM Almaden Research Center, 650 Harry Road, San Jose, California 95120

Received June 21, 2002; Revised Manuscript Received August 15, 2002

ABSTRACT: The dissolution of exposed regions of polymeric resists in aqueous base to form a pattern is a complex reactive process. It has recently been proposed that a critical level of ionization is required for a polymer chain to move from the film into solution. That model successfully predicts many of the features of polymer dissolution such as dependence on chain length and solution pH but has not been used to describe the detailed kinetics of the dissolution process. In this work we use the critical ionization model as a framework for a simple reaction scheme that describes the coupled reversible ionization−relaxation steps that transform a polymer chain from an unsolvated form into a solvated one. Simulations of the dissolution process are used to predict line shapes as a function of local extent of polymer deprotection in chemically amplified positive tone photoresists and examine chemical factors that lead to roughening. The results show that nonlinearities inherent in the dissolution kinetics are responsible for resist imaging. The kinetics also lead to increased roughening as the aerial image contrast is decreased. Implications of these results for current models of resist development and roughening are discussed. A kinetic criterion connecting critical ionization to the state of the materials in solid and solvated phases is proposed.

Introduction

Printed resist latent images are transformed into three-dimensional images by a wet development process that selectively removes soluble polymer chains.[1] This is a complex reaction−diffusion process that involves permeation of the resist film by the developer solution, transformation of polymer chains into a solvated form, and migration of the solvated chains into the bulk liquid.[2] The local dissolution rate depends on the extent of deprotection of the polymer (for positive tone resists) or its extent of cross-linking among chains (for negative tone resists). Much of the current practical description of this process stems from phenomenological models developed for positive tone Novolac-based resists. These models treat dissolution using parameters to build in selectivity for exposed regions and tie the overall rate to experiment.[3,4] The models are also applied to modern chemically amplified photoresists, which are very different chemical systems, with varying levels of success.[4]

Several physically realistic, molecular scale models of polymer dissolution have been proposed. Models originally developed for drug delivery polymers have been applied, providing a conceptual framework distinguishing stages of solvent permeation, polymer solvation and swelling (gelation), molecular disentanglement, and diffusion away from the film surface.[2,5] The dissolution rate of a resist has also been described as being controlled by a percolation process in which molecular fluctuations transport base ions from the solution along the polymer chains,[6] and the steady-state gel formation/dissolution process resulting from base permeation and reaction has been described.[7] These approaches all consider the development process to be governed by essentially mechanical phenomena involving diffusion of ions and water, relaxation, and disentanglement. Only one model has explicitly treated development as a reactive process: the critical ionization (CI) model, which successfully predicts the dependence of the dissolution rate on pH, ionic strength, molecular weight, and other factors.[8−10] Its basic assumptions are that the kinetics of the dissolution process are determined by the process of ionization and desorption of the ionized polymer molecule from the resist surface, which requires a certain minimum extent of ionization to enable detachment of the polymer from the film and movement into the basic solution. Within this framework, the dissolution mechanism is simply written as a series of desorption steps for polymer chains with at least the critical number of ionized sites. The rate of each step is of the form $R_i = k_{\mathrm{des},i}[\mathrm{P}_X\mathrm{H}_{X-i}{}^{i-}]$, where k_{des} is the desorption rate constant and $\mathrm{P}_X\mathrm{H}_{X-i}{}^{i-}$ is the polymer with i ionized sites, formed via a very fast acid−base equilibrium. Developer penetration is assumed to be insignificant, and solvation kinetics are neglected. These assumptions stem from treatment of resist dissolution as a process analogous to copper etching in aqueous acid and the commonly held belief that gelation in certain resist polymers is negligible. The CI model was developed for Novolac and hydroxystyrene (HOST) homopolymers. It was subsequently adapted to simulate dissolution of a partially deprotected Novolac resist polymer using either a continuum or a lattice to represent the repeat units.[11] While the CI model has proven to be very successful, application of the model in its original form to predict, for example, a resist image as a function of develop time, dose, and local polymer chemical composition requires estimates of desorption rates for each type of polymer chain, a formidable challenge for all but the simplest systems.

In addition to predicting resist profiles and rates, it is highly desirable that all models, physically based or phenomenonological, provide quantitative treatments of other aspects of development such as roughening, which may limit the usefulness of nanoscale lithography. Current minimum values for line edge roughness of developed features in positive tone chemically amplified resist systems are about 4−6 nm rms, essentially independent of line width.[12] Future lithography require-

* Corresponding authors: e-mail houle@almaden.ibm.com or hnsbrg@almaden.ibm.com.

10.1021/ma0209702 CCC: $22.00
Published on Web 09/25/2002

ments for semiconductors reduce the allowable roughness to 1−2 nm rms for feature sizes in the range 20−50 nm.[13] This degree of roughness is on the order of the molecular size.[14] One approach has been to connect roughening with the arrangement of molecules within the resist film that results in regions of varying solubility.[15,16] These configurations can be built in during coating or result from changes during the postexposure processing steps. Another has been to consider the statistical nature of the exposure and development steps which would result in chemical inhomogeneities within the resist and simulate profiles using a combination of molecular level and empirical models.[10,17,18] In this case roughness arises directly from normal local variations in extent of deprotection obtained with different exposure conditions. Roughness has also been linked to the statistics of chain removal within either the CI model[19] or the percolation model.[20]

All of these approaches to describing dissolution rates or roughening are dependent on knowing numerous details about complex systems or only partly describe the physical processes involved. None examines how the chemical composition of the exposed resist after postexposure bake, and detailed kinetics of the ionization and solubilization processes affect and control development. Clearly, it is vital to refine models of the physical picture of resist dissolution in order to assess the propensity of specific resist systems to develop roughening as well as to be able to predict other aspects of image quality. It is also necessary to develop models that can predict pattern topography for specific resist and developer formulations. In this work we present the first purely chemical kinetics-based model for resist polymer dissolution. The core assumption is that the CI model applies; that is, a critical level of ionization is required for solubilization. In recognition that gelation is inherent in polymer dissolution, even in phenolic polymers that are the basis for many modern resists,[21] we do not assume that purely surface processes dominate dissolution kinetics. We also consider base penetration to be more complex than percolation,[6] involving simultaneous hydration and polymer relaxation.[2,5,22,23] We recast the CI kinetics to incorporate characteristics of polymer reactive dissolution. Rather than separating ionization and desorption from the resist surface, we invoke a seamless process of penetration of the developer solution, ionization, solvation, and weakening of the polymer−polymer interaction to the point that migration of the molecule away from the film surface takes place. A schematic depicting the physical picture we have pursued is shown in Figure 1. We treat each polymer chain as a connected assembly of monomers that react independently, an approximation that is valid for HOST-based materials.[8,9] Thus, polymer ionization kinetics are assumed to include structural reorientation to accommodate water solvation and balancing of charge by a counterion.[5,22,23] Although our model is intended to be generic at this stage in order to explore its properties and predictions, we have scaled the overall dissolution rate predicted by the mechanism to fit experimental measurements for fully deprotected *p-tert*-butyloxycarbonyloxystyrene (PTBOCST) resist. This confers a realistic time scale on the simulated dissolution process and is consistent with our use of predicted latent images for the same resist system as input to the calculations.

By working within the basic assumption of the CI model and connecting the simulation time base to

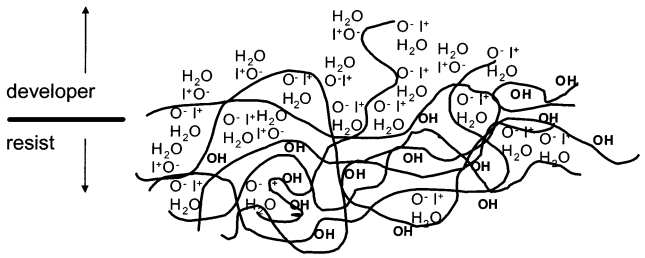

Figure 1. Schematic of a positive tone resist surface as dissolution takes place. The solubility of the resist is assumed to be governed by the formation of OH groups by a deprotection reaction. As developer solution penetrates the near-surface region of the polymer, basic anions extract protons to form O^- sites which are instantaneously balanced by positive counterions, I^+, and solvated with water. The polymer chains reorient and expand to accommodate the newly incorporated species and to stabilize the new charge distribution in the pendant groups. Microscopically, there is no distinct boundary between resist and solution.

experiment, we actually are probing the extendability of critical ionization to predict one-dimensional resist image formation in real time, thus gaining insight into the origins of resist contrast for various exposure conditions. We have also used the kinetic model to simulate development as a function of aerial image contrast in order to investigate its predictions concerning the connection between local extent of deprotection in the resist and roughening. This treatment is founded on observations that increasing roughness is linked to degradations in aerial image contrast, that is, degree of illumination of nominally unilluminated areas of the resist due to diffracted or scattered light or optical aberrations.[24,25] Because of the nonlinear nature of the chemical amplification process,[26] a reduction in image contrast leads to an increased fraction of the resist being subjected to marginal levels of light, where statistical effects in local deprotection yields would be most important.

Experiment

The dissolution time for 100% deprotected *p-tert*-butyloxycarbonyloxystyrene with *tert*-butyliodonium perfluorobutanesulfonic (TBI−PFBS) acid photoacid generator in Microposit MF CD26 developer (Shipley) was measured using a quartz crystal microbalance. The resulting product is described as poly-HOST (PHOST) but is not chemically identical to it because of side reactions that occur during deprotection.[27] The resist was prepared as described in an earlier study,[28] coated onto a quartz crystal, exposed to 200 mJ/cm^2 of 254 nm light, and baked at 100 °C for 90 s. The polymer was supplied by Kodak and had a molecular weight of approximately 52 000 amu and chain length of about 230 repeat units. The developer was used as supplied. The dissolution curve obtained is similar to those reported elsewhere,[29] with a thickness of 1 μm dissolving in approximately 8 s. The dissolution time was used to establish an absolute reference value to scale all the relative rate constants used in the mechanism in order to provide a realistic time scale to the simulated reactions. Measurements of trends in line-edge roughness with image contrast have been reported previously.[24]

Model

The latent image, formed by deprotected regions in the resist, that was used for the development simulations was predicted by a simulation of postexpose baked (PEB) PTBOCST/TBI−PFBS resist.[28,30] The film geometry for the PEB simulations, illustrated in Figure 2, uses a slab with a depth of 500 nm and a thickness of

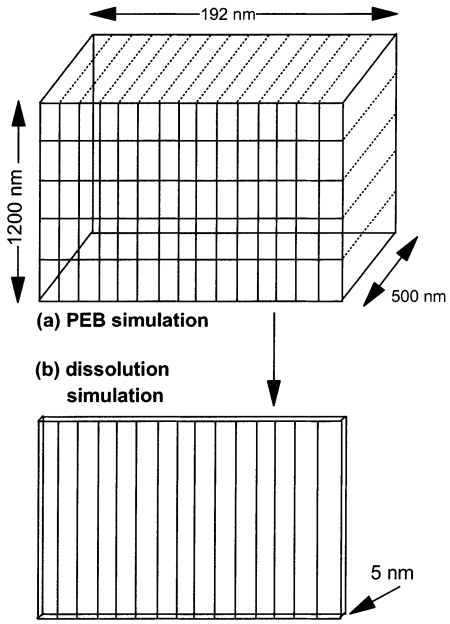

Figure 2. Simulation geometries used in this work. Both are for one period of a 192 nm line-space array in 1200 nm thick resist. They differ in their depth and volume element configurations.

1200 nm imprinted with a 1:1 192 nm pitch line-space array. The film is described using a single period of the array (extended through periodic boundary conditions) divided into 15 vertical and 5 horizontal slices, 75 volume elements total. The mechanism used in the PEB simulations is a description of the physics and chemistry of the imaging process in the resist and has been verified experimentally.[26,28,30] The specific simulation conditions used were an incident dose of 6.25 mJ/cm^2 followed by PEB at 100 °C for 120 s, corresponding to typical imaging conditions for PTBOCST resist. The output of the PEB simulations provides a spatial map of extent of deprotection, shown in Figure 3 together with the initial acid image, using concentrations of the pendant groups TBOCST and its deprotection product HOST to quantify local polymer stoichiometry.

The stoichiometries are converted to polymer chain distributions and used as input for dissolution simulations. As currently written, the simulation code[28] will only support top-down dissolution; that is, dissolution in a direction normal to the resist sidewalls is neglected. Although the simulator is not yet capable of predicting full dissolution, it is nevertheless useful for exploration and development of the basic dissolution algorithm and examining trends in film topography.

Resist Film Composition: Chemistry and Geometry of the Latent Image. The geometry used for the line-space array PEB simulations[28] was converted to a 1-D form for dissolution as shown in Figure 2. The horizontal divisions were eliminated by adding the final amounts of TBOCST and HOST in each of the 15 vertical stacks together and calculating the resulting concentrations. Since roughening of resists is on a nanometer scale, the slab depth was reduced from 500 to 5 nm. The concentrations remain the same because the material within each volume element is assumed to be homogeneous. Using the density for PTBOCST, 5.91 mol/L,[26] each volume element initially contains approximately 2.6×10^5 TBOCST groups. To define a surface region in contact with developer, a fixed amount of the material initially present, 1.3×10^4 groups, was defined as surface polymer chains. This corresponds to about 60 nm for PTBOCST homopolymer.[26] The remaining 1140 nm was bulk. The selection of a value of 60 nm is arbitrary but not unreasonable for phenolic materials which form measurable but thin gel layers in developer.[21a] Materials in which swelling is appreciable and comparable in rate to dissolution would require a more refined description. Aside from the definition of the surface region, the film is assumed to be structurally homogeneous throughout its thickess; that is, interfacial molecular mobility and morphology are ignored.[30,31]

Conversion of TBOCST and HOST Concentrations into Polymer Chains. Composition maps (Figure 3) are calculated without regard to connectivity of the TBOCST and HOST units. To use them as input for a dissolution simulation requires that these groups first be distributed among polymer chains. Since the goal of this work is to develop a description of the chemical kinetics of the critical ionization process and to understand its implications for resist development, as a first approximation the polymeric structure of the resist is treated at a highly simplified level. We have assumed that the polymer chains are monodisperse 10-mers, a size on the low end of the range used in chemically amplified resists.[14] The selection of this chain length should be viewed only as a construct. By scaling the rate constants of the 10-mers to match experimental data for a polymer containing about 230 repeat units, each monomer in the simulation has been tuned to represent a subset of 23 monomers (not necessarily contiguous) in the actual resist material. This permits the mechanism to be fine-grained enough to explore key aspects of resist dissolution but is not so detailed that the simulations become prohibitively complex. We do not expect that the use of longer polymer chains in the simulations will reveal qualitatively new trends. Partly deprotected chains are assumed to have random sequences of TBOCST and HOST groups.

The TBOCST:HOST stoichiometries in each volume element are converted to polymer chains using a Chemical Kinetics Simulator (CKS) simulation[32,33] that randomly distributes the monomers among the chains. This is accomplished using a hypothetical reaction scheme with steps of the general form

$$T_{10-x}H_x + T_{8-y}H_{y+2} \rightleftharpoons T_{9-x}H_{x+1} + T_{9-y}H_{y+1} \quad (1)$$

where T is a TBOCST group, H is a HOST group, x ranges from 0 to 10, and y ranges from 8 to 0. The forward and reverse rate constants in the equilibria are given by the statistical factors for the two steps: $k_f = (10 - x)(2 + y)$ and $k_r = (9 - y)(x + 1)$. Care is taken to eliminate mirror-image equilibria in order that the final distributions not be overweighted by multiple paths involving the same stoichiometries. The initial concentrations of $T_{10}H_0$ and T_0H_{10} are taken to be the final concentrations of TBOCST and HOST, respectively, in each volume element as obtained from the PEB simulations. The output is a distribution of 10-mers of varying composition, as shown in Figure 4, that correctly resolve to the initial TBOCST and HOST concentrations.

Dissolution Mechanism. The dissolution reaction mechanism used in this work is an extension of the CI model.[8,9] As originally described, this model presumes that all reversible ionization steps are at equilibrium and that the rate of dissolution is finite only for polymer chains with an ionization level at or above a minimum

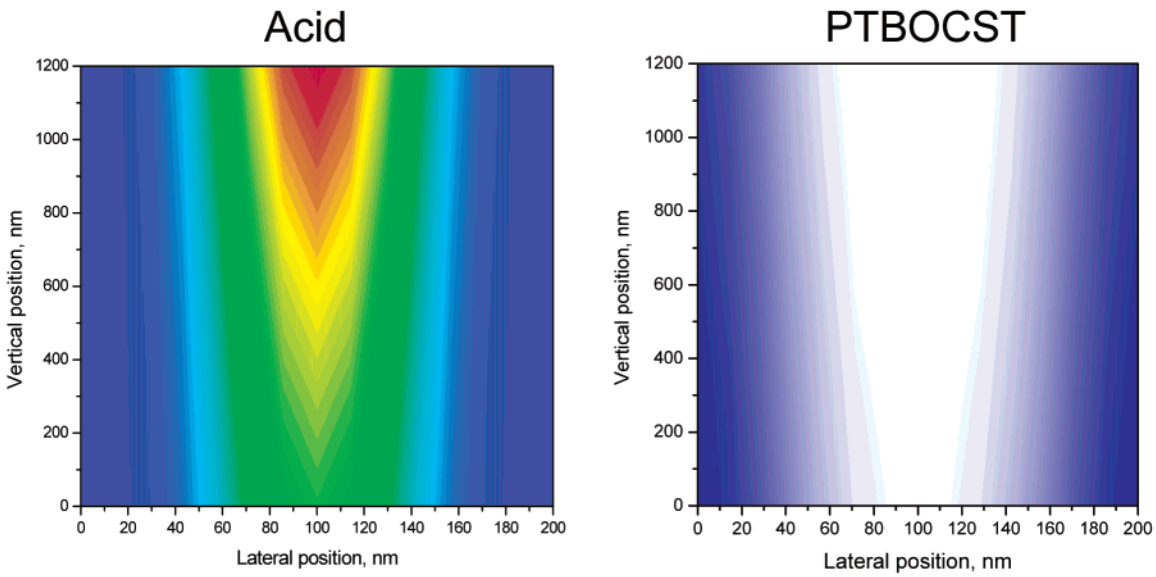

Figure 3. Maps of the calculated initial acid and final PTBOCST distributions used to prepare input for dissolution simulations. The PEB simulations were carried out for the geometry shown in Figure 2. The color scale for the acid map ranges from blue (zero acid) to red (1.12×10^{-2} mol/L). The color scale for the PTBOCST map ranges from blue (100%, 5.91 mol/L) to white (zero PTBOCST).

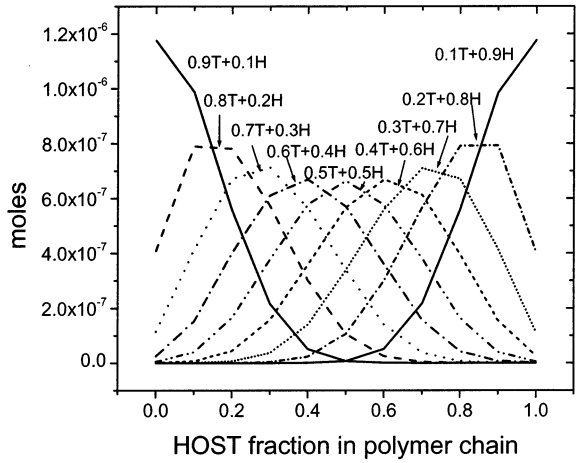

Figure 4. Distributions of 10-mer chain compositions obtained from the various initial film stoichiometries given in the figure labels. T is TBOCST, and H is HOST.

value. Although this construct is useful mathematically and has been very successful for explaining observed phenomena such as the developer strength dependence of polymer solubility,[8] it does not contain information on the complete kinetic path actually followed during dissolution.

It is this aspect of the CI model that we explore. We seek to develop a physically realistic CI dissolution mechanism that is as simple as possible, extendable to many types of polymers, predicts experimentally observed characteristics of resist development, and can be readily extended to incorporate new physics and chemistry as required.

The general form of the reaction scheme used here is step-by-step ionization to the critical level, followed by very rapid dissolution. Although the steps are simple in form, they represent a series of complex processes. We propose that in reality ionization and dissolution are not cleanly separable and have recently obtained experimental data that suggest this is a useful way of thinking about the dissolution process.[21] Each ionization step is not simple charge transfer but involves extraction of a proton by base, association of the anionic group and a positive counterion to maintain neutrality, solvation with water, relaxation of the ionized site to its new minimum-energy conformation, and reorientation of the local polymer chains to accommodate the new local composition.[2,5,22,23] As successively greater fractions of sites are ionized on a given chain, it becomes surrounded by water[22] and interacts less directly with other polymer molecules (see Figure 1). We propose that *the critical ionization threshold corresponds to a state in which the energy of the ionized and solvated state in the polymer film has become very close to the energy of an ionized molecule in solution*. At this point entropy will drive disentanglement and migration of the polymer chain into the liquid phase if the final ionized state persists long enough (reversal of ionization leading to neutralization is allowed). The steps are written as

$$T_{w\le5}H_{v\ge5} + OH^- \rightleftharpoons T_{w\le5}H_{v\ge4}I^- + H_2O \quad (2)$$

$$T_{w\le5}H_{v\ge4}I^- + OH^- \rightleftharpoons T_{w\le5}H_{v\ge3}I_2^- + H_2O \quad (3)$$

...

$$T_{w\le5}H_{v\ge1}I_4^- + OH^- \rightleftharpoons T_{w\le5}H_{v\ge0}I_5^- + H_2O \quad (4)$$

$$T_{w\le5}H_{v\ge0}I_5^- \rightarrow \text{dissolved} \quad (5)$$

where I is an ionized HOST group and $w + v = 10$. The CI level has not been determined for the various partially deprotected PTBOCST chains resulting from resist imaging, so we have assumed that it is 50%, i.e., only chains containing at least five HOST groups can be dissolved, a reasonable value.[9,10] In these simulations the core mechanism is a set of 66 reaction steps: five pairs of reversible ionization−neutralization steps and one dissolution step for the soluble polymer chain stoichiometries T_0H_{10}, T_1H_9, T_2H_8, T_3H_7, T_4H_6, and T_5H_5. A detailed discussion of how the rate constants for each step are determined is presented below.

The reaction sequence ends at the critically ionized level because we assume that the number of molecules

ionized to a greater extent and lingering at the surface of the resist film is kinetically insignificant. This is a different treatment than that presented previously,[9] which considered the dissolution rate to be governed by polymer chains whose CI levels exceeded the minimum. Our assumption allows some simplification of the dissolution reaction scheme, and tests of it indicate that it is not a drastic approximation at this stage. The kinetics are assumed to be pseudo-first-order in HOST; that is, the solution does not become depleted in OH^- during the dissolution process. (This would only hold for stirred or flowing developer or very large $[OH^-]$.) We also assume that there is no correlation between reactions involving adjacent pendant groups forcing a particular deprotection sequence. This is a reasonable assumption for HOST-based materials.[9] This model assumes nothing about structure of the solution at the resist surface or transport through solution.[5,10] Any impact of these factors on the kinetics is implicitly lumped into the rate constants for the individual steps.

Additional steps are included in the mechanism to describe the separate evolution of the surface and bulk regions of the portion of the resist film contained within each of the 15 volume elements. All dissolution reactions are assumed to involve only polymer chains designated as surface chains while the bulk acts as a reservoir. As each chain in the surface region dissolves, it is replaced by a chain randomly selected from the bulk (i.e., not necessarily of the same composition as the chain that had just been removed). This process keeps the amount of surface material constant until all bulk polymer had been consumed, at which point the surface material is eroded.

The molar densities (moles per unit volume) of the remaining polymer chains determine the thickness of the resist film as dissolution takes place and are necessary for the kinetics of the dissolution reaction to be accurate as the resist thins and concentrations of the various types of polymer chains change. Densities of chains of each stoichiometry were estimated from the known molar densities[26] of PTBOCST and PHOST using weighted sums.

Short lines (30 nm long) were pieced together from six dissolution simulations using identical starting concentrations but different random numbers. This permitted assessment of the degree of variation in developed resist profile due to statistical variations in the instantaneous ionization and dissolution rates.

Rate Constants. Within the reaction framework given here, the forward and reverse rate constants for steps 2−4 are composite quantities that fold together a variety of processes, scaled by a statistical factor σ representing the number of equivalent pathways open for each step. The statistical factors can be used to establish relative rate constants. As an example, in the case of the first pair of steps for the ionization−neutralization sequence of a 10-HOST chain,

$$T_0H_{10} + OH^- \rightleftharpoons T_0H_9I_1^- + H_2O \qquad (6)$$

there are 10 ways to ionize T_0H_{10} and one way to neutralize $T_0H_9I_1^-$, so the statistical factors are 10 in the forward direction and 1 in reverse. The next pair of steps interconverts $T_0H_9I_1^-$ and $T_0H_8I_2^-$ and has forward and reverse statistical factors of 9 and 2, respectively. Continuing this pattern, the final pair of steps,

$$T_0H_6I_4^- + OH^- \rightleftharpoons T_0H_5I_5^- + H_2O \qquad (7)$$

has statistical factors of 6 and 5. If the initial polymer is not fully deprotected and has, for example, a composition that is 40% TBOC and 60% HOST, the statistical factors for its steps would be appropriately modified. In this case the forward and reverse factors for the steps

$$T_4H_2I_4^- + OH^- \rightleftharpoons T_4H_1I_5^- + H_2O \qquad (8)$$

are 2 and 5.

Absolute numerical values for the rate constants for the full mechanism are unknown, so we have estimated them using the statistical factors. The equilibrium constants for each stage of ionization are predicted to differ only by statistical factors because of the minimal coupling between adjacent HOST pendant groups.[8] We assume this to be the same for our more complex description that also includes solvation and relaxation. The forward and reverse rate constants for the ith reversible pair of steps can therefore be written as $k_{f,i} = k\sigma_{f,i}$ and $k_{r,i} = k\sigma_{r,i}$, respectively, where k is constant for all the steps in the scheme. Since the values for $\sigma_{f,i}$ and $\sigma_{r,i}$ are readily determined for each step, the value for k can be found by scaling $k_{f,i}$ and $k_{r,i}$ for all i collectively to fit the experimental dissolution time for fully deprotected PTBOCST. The best fit value for k was found to be 2.16, leading to values of 21.6 and 2.16 for $k_{f,i}$ and $k_{r,i}$ in steps (6) and 4.32 and 10.8 in steps (8). The rate constant for steps of type (5) was set at an arbitrary large value because their kinetic purpose is essentially bookkeeping: once the polymer has reached its critically ionized state and persists for a sufficiently long time without being reneutralized, it can be considered to be irreversibly detached from the polymer film. The rate constants can be modified to include effects such as varying polymer molecular weight or developer concentration by rescaling k to match the appropriate experimental data.

Simulations Using Degraded Contrast Aerial Images. Contrast in patterned illumination is defined here as $C = (I_{max} - I_{min})/I_{max}$, where I_{max} and I_{min} are the maximum and minimum light intensities. It has been shown experimentally that as contrast decreases, line edge roughness increases.[24,34] The simulations described earlier in this section assume 100% contrast. We have carried out PEB simulations for a range of degraded contrasts (61%, 49%, 36%, and 10%),[24] with the balance between modulated and background illumination chosen to keep dose constant at line edges. These simulations explore the interaction between degraded image contrast and dissolution kinetics to produce a specific resist image. The initial acid concentrations used for the postexpose bake simulations are shown in Figure 5.

Statistical Effects. The simulation code used in this study models chemical reactions by random selection of probability-weighted events.[35] The event selection sequence depends on the random number sequence used. This characteristic allows statistical effects on local events to be readily assessed simply by running a set of otherwise identical simulations with differing random number seeds. We performed a series of such simulations for each of the five contrast cases investigated in this work in order to explore the connection between dissolution kinetics and roughening. As shown in Figure 2, the slab geometry for each case was 192

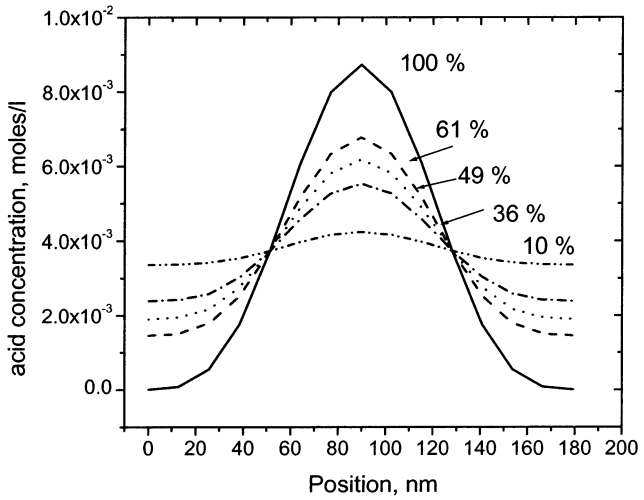

Figure 5. Initial acid latent images with varying contrast for PEB simulations using the 5-layer, 15-slice geometry. Plots are shown for the top layer of the resist volume only; images in the other four layers are attenuated due to the optical absorbance of the polymer. The mixture of modulated and background illumination was chosen to keep dose constant at the line edges.

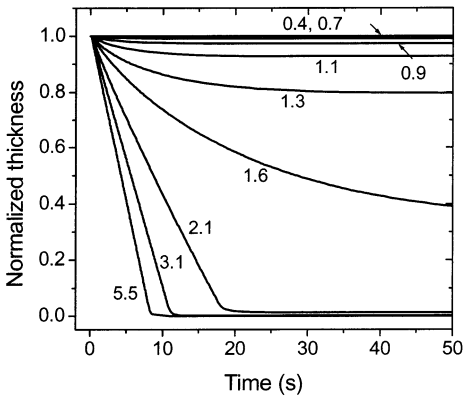

Figure 6. Resist thickness as a function of absorbed dose (in mJ/cm^2) and time.

nm wide × 1200 nm thick × 5 nm deep. By abutting six slabs calculated using the same initial acid profile but different random number seeds, we constructed 30 nm line segments. Although short, these were useful for qualitative assessment of topography trends.

Results

Characteristics of the Dissolution Process. As an initial exercise, the characteristics of the dissolution model were explored for unpatterned films with stoichiometries ranging from 100% HOST to 10% HOST. These compositions are expected for an absorbed dose range of 0.2−6 mJ/cm^2. The initial polymer chain distributions for each stoichiometry are shown in Figure 4. Simulations were run until the dissolution reaction was complete; that is, the resist film thickness reached a limiting value. Results to 50 s are shown in Figure 6. They are replotted as a contrast curve in Figure 7. The value $\gamma = 4.2$ predicted by the simulations is comparable to those measured for TBOCST−HOST copolymer resists.[36]

To connect the extent of dissolution as a function of dose more closely to the chemical kinetics of the process, Figure 8 presents the same simulation results as a function of HOST fraction together with the times

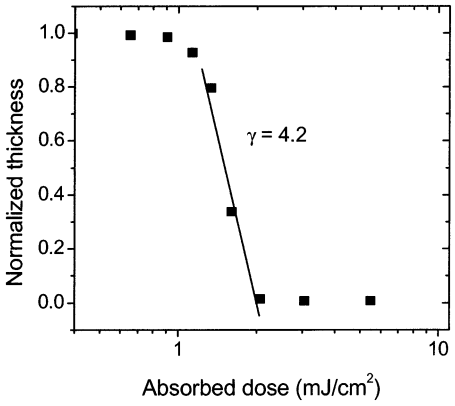

Figure 7. Resist contrast as a function of absorbed dose.

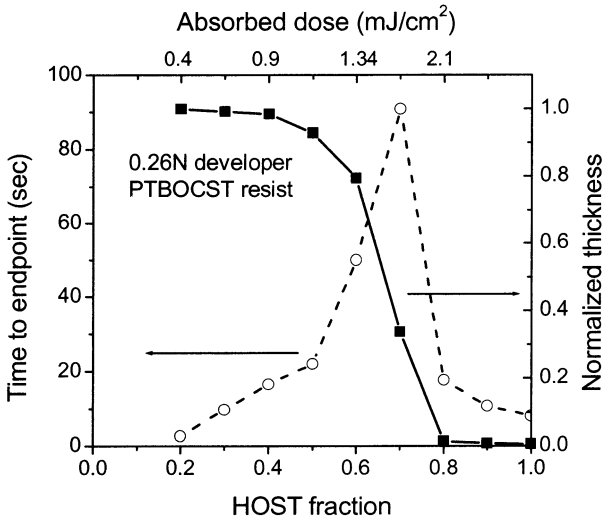

Figure 8. Results of unpatterned film dissolution simulations for a range of HOST fractions.

required for films containing each HOST concentration level to reach their final thicknesses. The elapsed time is short when the HOST fraction is low because there is little to dissolve, reaches a maximum at a HOST fraction of 70%, and then rapidly declines as the dissolution rate becomes very fast. It is this latter part of the curve that is important: nonlinearity in the dissolution behavior arises naturally from the simple reversible ionization kinetics and the CI framework used in this study. There is a clear breakpoint in solubility at the 80% HOST concentration level. Interestingly, this corresponds to generally used rule of thumb that 80% deprotection levels are required for complete resist solubility. This result should be viewed as a coincidence given the crudeness of our model, but observation of a trend in qualitative alignment with experiment is an indication that we are thinking correctly about the development process.

As described in the Model section, the film is divided into a surface region that interacts with the developer and a bulk region. As surface chains are dissolved, they are randomly replaced by chains from the bulk. Not all the surface chains will meet the CI criterion for solubility, set to be 50% HOST in this work, and those with the minimum level of deprotection will only dissolve slowly because of the number of reversible ionization steps involved. Eventually a layer of less soluble or insoluble chains will build up in the surface region. Although it is possible that these could be carried away by dissolution of underlying material, this process could

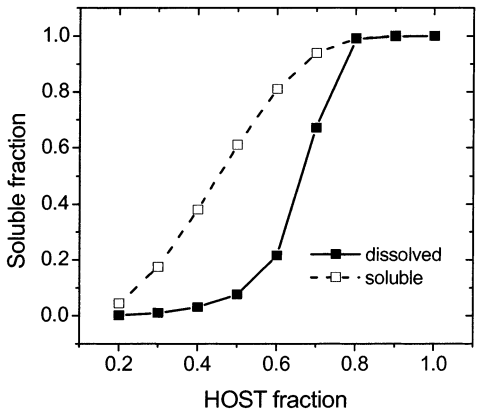

Figure 9. Comparison of dissolved and soluble components for films with a range of HOST fractions. The total amount of soluble material was determined by adding concentrations of all chains with HOST fractions >0.5 for each stoichiometry.

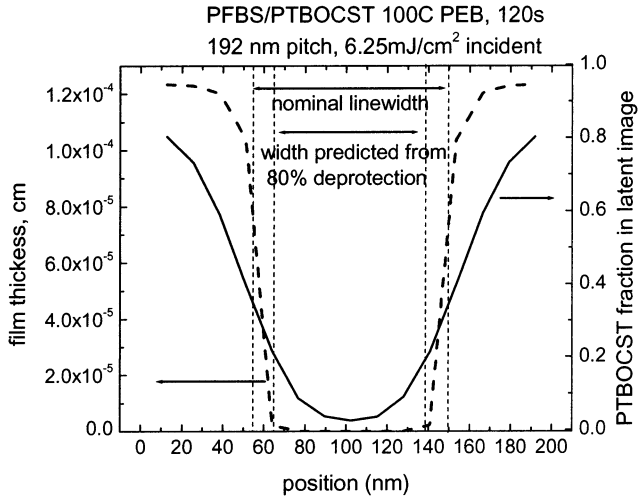

Figure 10. Predicted developed profile (dashed line) obtained using the latent image from a PEB simulation (solid line). The resist was PFBS/PTBOCST, exposed with an incident dose of 6.25 mJ/cm^2 at 192 nm pitch, 100% contrast, and baked at 100 °C for 120 s. The development time was 90 s. Also shown are line widths predicted from the pitch and from the location of deprotected material exceeding 80% HOST.

not be included in our 1-D model in a straightforward way. Nevertheless, it is interesting to note that accumulation of insoluble material is predicted and, as shown in Figure 9, is also associated with nonlinearity in the dissolution process. The importance of this phenomenon and its connection to the long time required for dissolution to reach completion remains to be investigated experimentally.

Development of a 192 nm Pitch Line-Space Array at 100% Aerial Image Contrast. Dissolution of a 192 nm pitch line-space array after PEB transforms the initially compositionally graded structure into a nearly straight-walled profile, as shown in Figure 10. The resulting line profile is compared to the nominal 96 nm width and to the width expected from the rule of thumb that all material deprotected to an average of 80% will dissolve and is seen to span both.

Effect of Contrast Degradation on Developed Profiles. Figure 11 presents simulated profiles for latent images obtained assuming 61%, 49%, 36%, and 10% aerial image contrast, to be compared to Figure 10. The primary impact of contrast loss is resist line-narrowing and thickness loss. Interestingly, although the final resist image varies substantially as contrast is degraded, imaging persists to a contrast as low as 36%. The image is lost altogether at 10% contrast. This observation is in agreement with trends seen in experiment.[24]

Roughening as a Function of Contrast. To assess the connection between roughening and dissolution statistics, resist lines were constructed as described in the Model section. Because the scale of the roughening is much smaller than the characteristic size of the developed lines, it is not readily visualized using full scale plots. Therefore, we have plotted the simulation results as deviations from a local average thickness computed from the six simulations. The resulting maps are shown in Figure 12. There are two perspectives: the top-down view presents the line segment in its correct aspect ratio, while the 3-D view is expanded to allow detail to be seen more readily. It should be borne in mind that these are coarse-grained simulations, with each volume element representing a 5 × 13 nm area and each line structure containing 90 volume elements. Despite the low resolution, it is clear from the maps that roughening increases with decreasing aerial image contrast. The maps for 10% contrast are the smoothest; however, as seen in Figure 11 the resist is nearly all 80% deprotected, and very little material is left after development.

The simulation results are replotted in Figure 13 in the form of absolute thickness variation as a function of HOST fraction across the line for 100%, 61%, 49%, and 36% contrast. It is evident that the roughness peaks over a fairly narrow resist composition range, 0.5−0.7 HOST. As seen in Figures 7 and 8, these compositions correspond to the range over which the material is switching from soluble to insoluble, as is found at a line edge. A similar correlation between roughness and extent of deprotection, or dose, has been observed in previous studies.[37]

Discussion

Several resist dissolution models have used parametrized expressions to compute a dissolved fraction from the local imaged film composition, thereby generating an image.[3,4] More microscopic models focus on the polymer ionization process to describe the dependence of dissolution kinetics on process variables.[6,8−11] Polymer dissolution models consider the process of conversion of polymer molecules from the solid phase to a solvated phase as formation of a series of stacked layers with moving boundaries.[2,5,7] While all of these models are successful in describing various experimental observations, they each capture only part of the overall resist development process. The very simple model here is a new approach that has the potential for providing a unified description of resist pattern formation. Starting from the chemical steps of polymer ionization, solvation, and disengagement from the bulk, the model is able to predict profile and roughness evolution in real time and can connect profiles to the latent images resulting from exposure and PEB. pH, temperature, and polymer composition dependences are easily embodied in the kinetic mechanism through the rate constants, and their effects on feature profiles can be assessed in a straightforward way. Progressive formation and dissolution of intermediate layers such as gels is readily incorporated through the definition of the reaction mechanism and the selection of spatial scale of the geometric grid

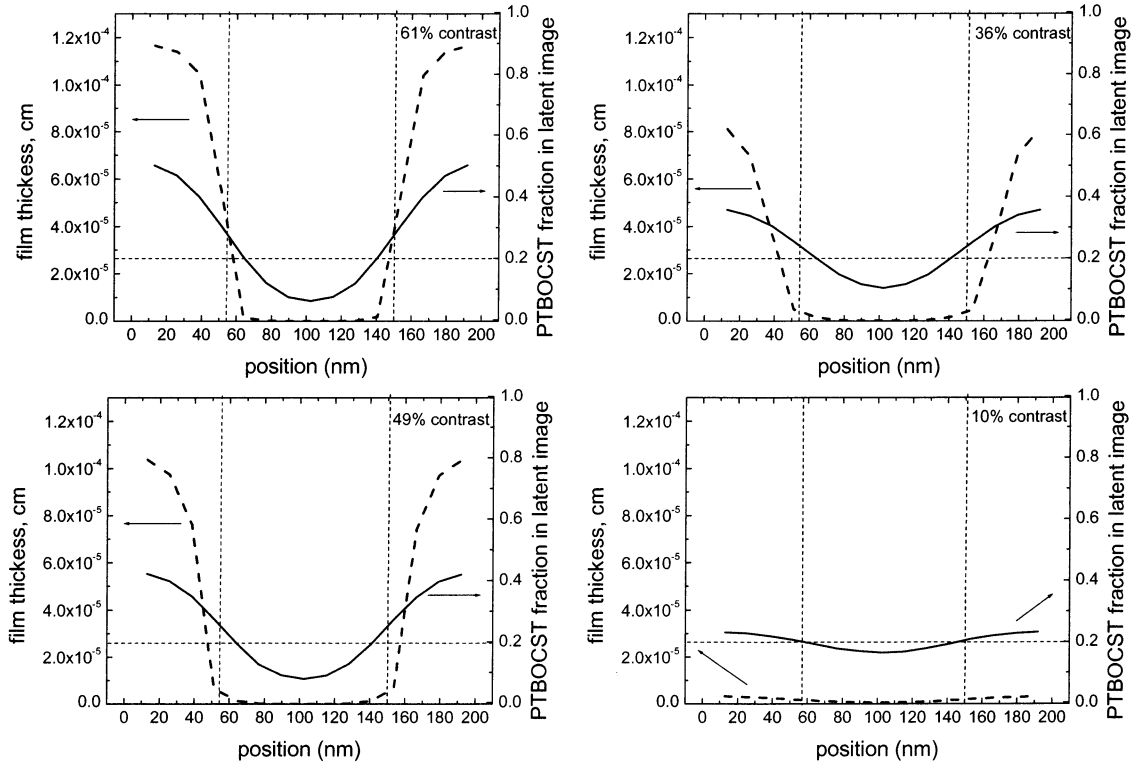

Figure 11. Plots of latent images and dissolution profiles for the same conditions as in Figure 8, except with 61%, 49%, 36%, and 10% contrast. The dashed vertical lines show the nominal line width, and the horizontal line shows the 80% deprotection level.

defined for the system, and the moving boundaries and variable volumes that result are easily treated in the stochastic formalism.[24,26,33,38]

There are two important aspects of resist dissolution that are not incorporated in the simulations but may have a significant effect on the results. These are dissolution in three dimensions and description of the internal structure of the polymer film. The frequency spectrum of the roughening should be quite sensitive to the dimensionality of dissolution, but the trends in roughness amplitude with image contrast are likely to be unchanged. Incorporation of such phenomena as removal of insoluble material by entrainment with soluble material, which can be made possible in a 3D model, is important for capturing details of line shapes. There have been a number of proposals that roughening during dissolution is a consequence of compositional and morphological inhomogeneities that are present or formed in the resist film.[15,16] This can be incorporated by taking advantage of VSIM's capability to define separate chemistry for every volume element in the system.

Because it can predict nonlinearities and roughening observed in resist profiles with a minimum of assumptions, the very simple description of resist development presented in this work can be considered to capture much of the essential physics and chemistry of the dissolution process. The straight-walled profile that is formed from a diffuse latent image arises naturally from the kinetics used to represent the process of reversible ionization, neutralization, and solvation of acidic sites on each polymer chain. Regions with high concentrations of deprotected groups will have polymer chain composition distributions weighted toward completely soluble chains, i.e., chains with a fraction of ionizable groups well in excess of the minimum required by the CI framework. These dissolve quickly. As the extent of deprotection decreases at the edges of the developable latent image the fraction of insoluble chains increases, leading in time to an accumulation of insoluble material. Moreover, those chains that are soluble are only barely so: the ionization process is not only slower, but statistics favor neutralization. As illustrated in Figures 7−9, substantial nonlinearities in rate and solubility result.

These simulations only treat roughness that arises from a single initial deprotected polymer distribution. To develop a complete description of the roughening that arises from kinetics alone it is necessary to include statistical effects in the initial PAG photochemistry and the PEB chemistry. It should be noted that it is not inevitable that the contributions from these sources will dominate: a systematic study of line-edge roughening as a function of aerial image contrast and development conditions[12,24,39] has shown that there is no systematic trend in degree of roughness with resist type, only with developer concentration.

The model is an implementation of the critical ionization model, with an integrated description of the dissolution process. The underlying physical assumption is that the various steps involved in dissolution cannot be cleanly separated, following models for drug delivery.[5,22] In our picture, as ionization proceeds and progressively larger amounts of water surround the polymer chains, at some point the molecules will be energetically close to molecules in solution, and migration away from the resist surface will be driven by entropy and concentration gradients. In the mechanism, this stage is defined to be the 50% ionization point, but this is an arbitrary choice in this work. Knowledge of the critical ionization level for various polymers[10] and a characteristic dissolution time for a specific polymer

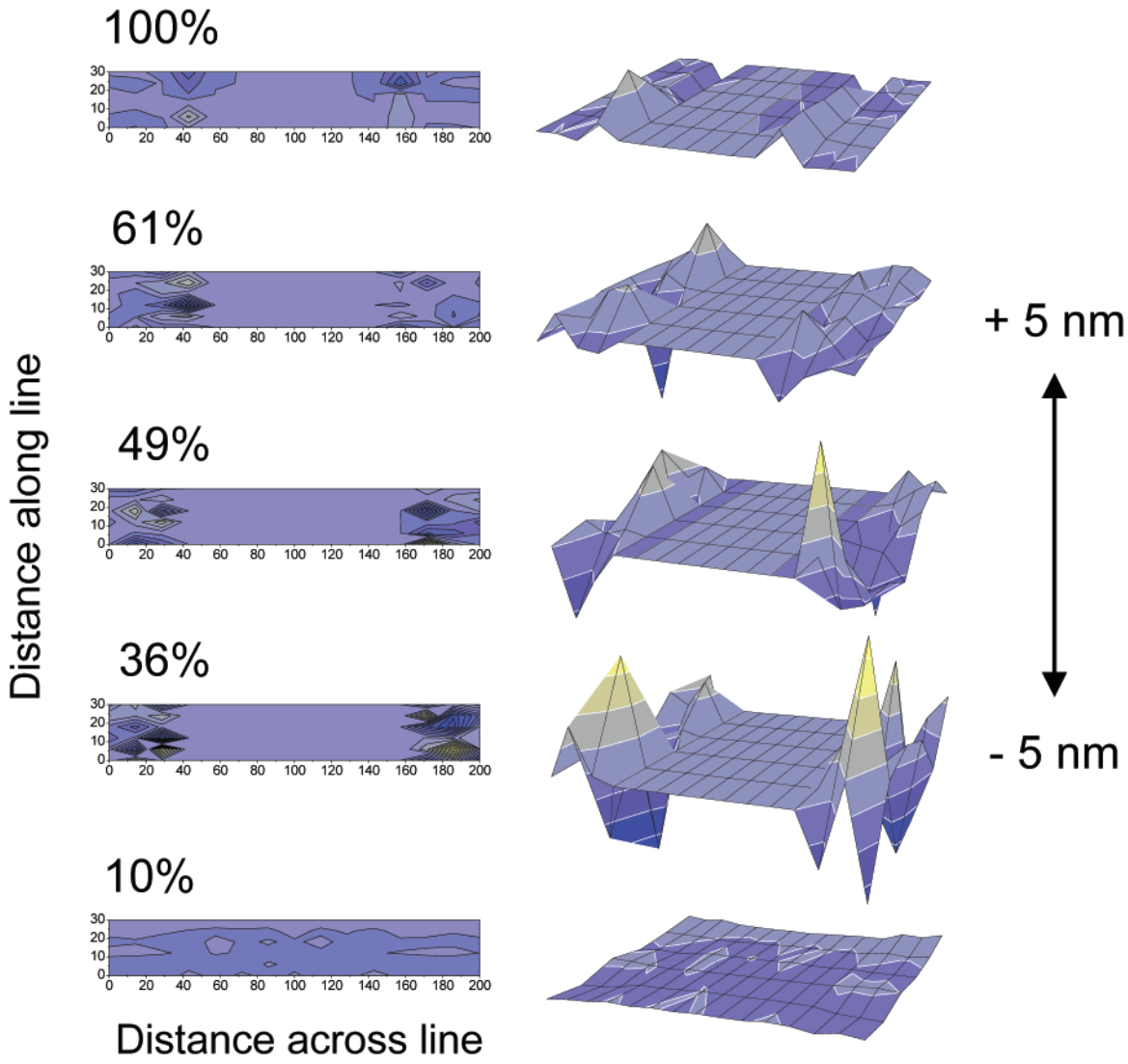

Figure 12. Maps of roughening during dissolution, computed as a deviation from average thickness. The top-down views on the left are drawn to scale, and the 3D views are expanded to facilitate visualization of details.

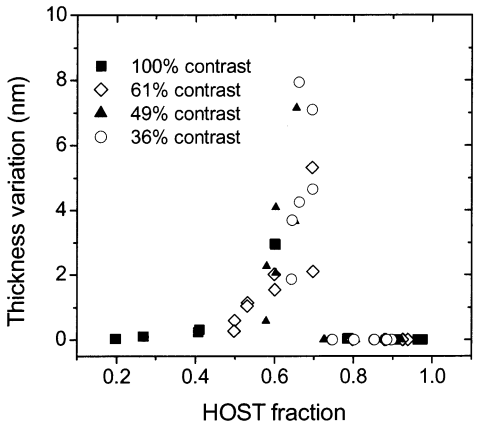

Figure 13. Variation in roughness as a function of extent of deprotection. Values were determined from the range of maximum and minimum thicknesses predicted by the six simulations used to compose line segments for each of the four contrast cases.

composition are the two pieces of information essential for successful application and extension of our model. Development of experimental and theoretical techniques to extract the critical ionization level as a function of polymer type and dissolution conditions and the resulting successful prediction of line profiles and other patterning results will provide a stringent test of our approach.

Conclusions

We present a kinetic model for photoresist dissolution built upon the critical ionization framework. The model considers the dissolution process to be a series of reversible monomer−centric ionization, solvation, and relaxation steps that convert dry polymer with a minimum degree of deprotection to dissolved chains. A one-dimensional implementation of the model is presented for PTBOCST, which deprotects to PHOST. The relative rates of the steps are determined by statistical factors, and the absolute rates are scaled to match the overall experimental dissolution time for fully deprotected PTBOCST. Generic simulations show that the kinetic model embodies important nonlinearities observed experimentally, such as selectivity for highly deprotected regions and roughening, suggesting that these are kinetic in origin. Application of the model to simulations of line profiles obtained from 192 nm line-space array latent images printed with varying aerial image contrast show that the predicted line width at the bottom of the features is the same as that expected assuming

that all resist with greater than 80% deprotection will dissolve. They also predict that roughening is sensitive to local stoichiometry and will increase as contrast degrades, in agreement with experiment. The model is readily extendable to 3 dimensions and can incorporate dynamic phenomena known to be important such as gelation.

Acknowledgment. We are grateful to Seok-Won Lee and Gregg Gallatin for many helpful discussions.

References and Notes

(1) Thompson, L. F., Willson, C. G., Bowden, M. J., Eds.; *Introduction to Microlithography*, 2nd ed; American Chemical Society: Washington, DC, 1994; Chapters 3 and 4.
(2) Narashimhan, B.; Peppas, N. A. *Adv. Polym. Sci. Polym. Anal. Polym. Phys.* **1997**, *128*, 157. Herman, M. F.; Edwards, S. F. *Macromolecules* **1990**, *23*, 3662.
(3) Arthur, G.; Mack, C. A.; Eilbeck, N.; Martin, B. *Microelectron. Eng.* **1998**, *41/42*, 311.
(4) Dammel, R. R.; Sagan, J. P.; Kokinda, E.; Eilbeck, N.; Mack, C. A.; Arthur, G. G.; Henderson, C. L.; Scheer, S. A.; Rathsack, B. M.; Willson, C. G. *SPIE Adv. Resist Technol. Proc. XV* **1998**, *3333*, 401.
(5) Narasimhan, B. *Adv. Drug Delivery Rev.* **2001**, *48*, 195.
(6) Shih, H.-Y.; Zhuang, H.; Reiser, A.; Teraoka, I.; Goodman, J.; Gallagher-Wetmore, P. M. *Macromolecules* **1998**, *31*, 1208.
(7) Choi, S. J.; Cho, J. Y. *SPIE Adv. Resist Technol. Proc. XIII* **2001**, *4345*, 952.
(8) Tsiartis, P. C.; Flanagin, L. W.; Henderson, C. L.; Hinsberg, W. D.; Sanchez, I. C.; Bonnecaze, R. T.; Willson, C. G. *Macromolecules* **1997**, *30*, 4656.
(9) Flanagin, L. W.; McAdams, C. L.; Hinsberg, W. D.; Sanchez, I. C.; Willson, C. G. *Macromolecules* **1999**, *32*, 5337.
(10) Burns, S. D.; Schmid, G. M.; Tsiartis, P. C.; Willson, C. G.; Flanagin, L. *J. Vac. Sci. Technol. B* **2002**, *20*, 537.
(11) Flanagin, L. W.; Singh, V. K.; Willson, C. G. *J. Polym. Sci., Part B: Polym. Phys.* **1999**, *37*, 2103.
(12) Sanchez, M. I.; Hinsberg, W. D.; Houle, F. A.; Hoffnagle, J., unpublished work, 2001. Data available on request.
(13) Levinson, H. *Solid State Technol.* **2002** (January), 36.
(14) Radius of gyration for molecular weights in the range of 1000−100 000 estimated using formulas in: Billmeyer, F. *Textbook of Polymer Science*, 2nd ed.; Wiley-Interscience: New York, 1984; pp 154−157.
(15) Yamaguchi, T.; Namatsu, H.; Nagase, M.; Yamazaki, K.; Kurihara, K. *Appl. Phys. Lett.* **1997**, *71*, 2388.
(16) Lin, Q.; Goldfarb, D.; Angelopoulos, M.; Sriram, S.; Moore, J. S. *SPIE Adv. Resist Technol. Proc. XVIII* **2001**, *4345*, 277.
(17) Schmid, G. M.; Smith, M. D.; Mack, C. A.; Singh, V. K.; Burns, S. D.; Willson, C. G. *SPIE Adv. Resist Technol. Proc. XVIII* **2001**, *4345*, 1037.
(18) Gallatin, G. *Proc. SPIE* **2001**, *4404*, 123.
(19) Flanagin, L. W.; Singh, V. K.; Willson, C. G. *J. Vac. Sci. Technol. B* **1999**, *17*, 1371.
(20) Patsis, G. P.; Glezos, N.; Raptis, I.; Valamontes, E. S. *J. Vac. Sci. Technol. B* **1999**, *17*, 3367.
(21) Hinsberg, W. D.; Lee, S. W.; Kanazawa, K. K., unpublished work, 2002. Data available on request. (b) Hinsberg, W. D.; Lee, S. W.; Kanazawa, K. K. *Anal. Chem.* **2002**, *74*, 125. Hinsberg, W. D.; Lee, S. W.; Horne, D.; Kanazawa, K. *SPIE Adv. Resist Technol. Proc. XVIII* **2001**, *4345*, 1.
(22) Heller, J.; Baker, R. W.; Gale, R. M.; Rodin, J. O. *J. Appl. Polym. Sci.* **1978**, *22*, 1991.
(23) Rossi, G.; Mazich, K. A. *Phys. Rev. E* **1993**, *48*, 1182.
(24) Hinsberg, W.; Houle, F. A.; Hoffnagle, J.; Sanchez, M.; Wallraff, G.; Morrison, M.; Frank, S. *J. Vac. Sci. Technol. B* **1998**, *16*, 3689.
(25) Shin, J.; Han, G.; Ma, Y.; Moloni, K.; Cerrina, F. *J. Vac. Sci. Technol.. B* **2001**, *19*, 2890.
(26) Wallraff, G.; Hutchinson, J.; Hinsberg, W.; Houle, F. A.; Seidel, P.; Johnson, R.; Oldham, W. *J. Vac. Sci. Technol. B* **1994**, *12*, 3857.
(27) Ito, H.; Sherwood, M. *SPIE Adv. Resist Technol. Proc. XVI* **1999**, *3678*, 104.
(28) Houle, F. A.; Hinsberg, W. D.; Morrison, M.; Wallraff, G.; Larson, C.; Sanchez, M. I.; Hoffnagle, J. *J. Vac. Sci. Technol. B* **2000**, *18*, 1874.
(29) Ito, H. *IBM J. Res. Develop.* **2001**, *45*, 683.
(30) Houle, F. A.; Hinsberg, W. D.; Sanchez, M. I.; Hoffnagle, J. A. *J. Vac. Sci. Technol.* **2002**, *20*, 924.
(31) Hall, D. B.; Torkelson, J. M. *Macromolecules* **1998**, *31*, 8817.
(32) Hinsberg, W. D.; Houle, F. A. Chemical Kinetics Simulator is available for a no-cost license from http:/www.almaden.ibm.com/st/msim.
(33) Houle, F. A.; Hinsberg, W. D. *Surf. Sci.* **1995**, *338*, 329.
(34) Shin, J.; Han, G.; Ma, Y.; Moloni, K.; Cerrina, F. *J. Vac. Sci. Technol. B* **2001**, *19*, 2890.
(35) Bunker, D. L.; Garrett, B.; Kleindienst, T.; Long, G. S., III. *Combust. Flame* **1974**, *23*, 373. Gillespie, D. *J. Comput. Phys.* **1976**, *22*, 403.
(36) Kumada, T.; Adachi, H.; Watanabe, H.; Sumitani, H. *SPIE Adv. Resist Technol. Proc. XIV* **1997**, *3049*, 459.
(37) He, D.; Cerrina, F. *J. Vac. Sci. Technol. B* **1998**, *16*, 3748.
(38) Houle, F. A.; Hinsberg, W. D. *Appl. Phys. A* **1998**, *66*, 143.
(39) Sanchez, M. I.; Hinsberg, W. D.; Houle, F. A.; Hoffnagle, J.; Ito, H.; Morrison, M. *SPIE Adv. Resist Technol. Proc. XVI* **1999**, *3678*, 160.

MA0209702